Preprints of the 21st IFAC World Congress (Virtual)
Berlin, Germany, July 12-17, 2020

Real-Time Solution to Quadratically Constrained Quadratic Programs for Predictive Converter Control

Zhe Chen [*], **Robin Verschueren, Stefan Almér** [**], and **Goran Banjac** [***]

[*] *École Polytechnique Fédérale de Lausanne, Lausanne, Switzerland. E-mail: zhe.chen@epfl.ch.*
[**] *ABB Corporate Research, Baden, Switzerland. E-mail: {stefan.almer, robin.verschueren}@ch.abb.com*
[***] *ETH Zurich, Zurich, Switzerland. E-mail: gbanjac@control.ee.ethz.ch*

Abstract: This paper considers the real-time implementation of MPC tailored to voltage source converters with inductive-capacitive filter. Previous work has shown that the nonlinear and non-convex MPC problem can be equivalently formulated as a convex quadratically constrained quadratic program (QCQP). We develop two tailored algorithms based on the OSQP and HPIPM solvers to efficiently solve this QCQP. As the aforementioned solvers do not support quadratic constraints, we extend them so that they can solve QCQPs. We provide numerical comparison between the proposed methods and state-of-the-art solvers and show that our solvers are suitable for embedded applications.

Keywords: Predictive control, Embedded systems, Inverters, Efficient algorithms, Operator splitting method, Riccati-based interior-point method.

1. INTRODUCTION

With the development of renewable energy, the modern power system is undergoing significant change with ever increasing presence of grid-connected power converters (Parvez et al., 2016). Model predictive control (MPC) has been applied for a wide range of converter control applications (Vazquez et al., 2016), and has shown to improve both dynamic performance and efficiency of converters, see *e.g.*, Spudić and Geyer (2017); Richter et al. (2016); Hokayem et al. (2014); Almér et al. (2013, 2015).

Application of MPC requires the solution of optimization problems in real time. The fast control frequencies of converters mean that the real-time optimization has to be performed at high speed. This is a challenging problem which has been the focus of a large body of work (Ferreau et al., 2017). A recent theoretical result has shown that for certain power converter topologies, the non-convex MPC problem can be equivalently reformulated as a convex quadratically constrained quadratic program (QCQP) with a certain structure (Almér et al., 2020). This result motivates further research into fast real-time optimization of QCQP, which is carried out in the present paper.

The solution to MPC problems can be computed with iterative optimization methods and solvers, *e.g.*, Richter et al. (2012); Domahidi et al. (2013, 2012). First-order methods exploit first-order information of the problem to iteratively compute an optimal solution. Operator splitting techniques are well-known first-order methods that formulate the optimization problem as a problem of finding a zero of the sum of monotone operators (Lions and Mercier, 1979; Douglas and Rachford, 1956). The alternating direction method of multipliers (ADMM) is a particular operator splitting method, which has been studied extensively (Gabay and Mercier, 1976; Glowinski, 1984; Eckstein and Bertsekas, 1992; Boyd et al., 2011). Due to its computationally cheap iterations and good practical convergence behavior, ADMM is well suited to embedded applications with limited computing resources wherein high accuracy solutions are typically not required due to noise in the data.

Very recently, a novel operator splitting method for quadratic programs based on ADMM was proposed (Stellato et al., 2020; Banjac et al., 2017, 2019). The method exploits a new splitting requiring the solution to a quasi-definite linear system. The method makes no assumptions on the problem data other than convexity. Furthermore, it can provide primal and dual infeasibility certificates if the problem is infeasible. Besides, warm starting can be easily integrated to reduce the number of iterations and if the problem matrices are time-invariant, the matrix factorization can be cached and reused multiple times to improve the computation time.

Another important class of optimization methods are interior-point methods. They are second-order methods for constrained optimization. An important method in this class is the Mehrotra predictor-corrector method (Mehrotra, 1992), a primal-dual interior-point method which is widely used in practical implementations due to the good performance across various problems (Wright, 1997).

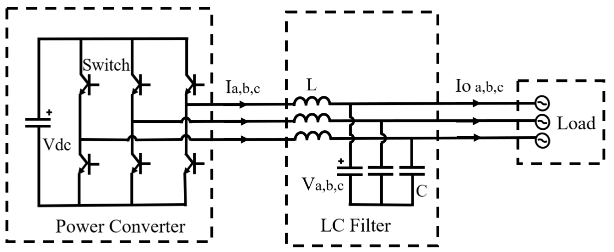

Fig. 1. Two level three-phase voltage source converter with LC filter

Recently, based on previous work (C.V.Rao et al., 1998), a predictor-corrector method for linear MPC addressed on a Riccati factorization was proposed (Frison and Jørgensen, 2013). An efficient implementation exists in the HPIPM package (Frison et al., 2014), which significantly improves performance for small to medium scale problems compared to other implementations of interior-point methods. An important part of the speedup comes from an optimized linear algebra implementation called BLASFEO (Frison et al., 2018).

This paper explores the real-time implementation of MPC tailored to voltage source converters with inductive-capacitive filter. Based on the previous work (Almér et al., 2020), where an equivalent formulation of MPC as a QCQP, we develop two tailored algorithms based on the OSQP and HPIPM solvers to efficiently solve this QCQP. As the aforementioned solvers do not support quadratic constraints, we extend them so that they can solve QCQPs. Besides, we provide numerical comparison between the proposed methods and state-of-the-art solvers and show that our solvers are suitable for embedded applications.

The content of the present paper is as follows. We discuss the problem setup and review the specific MPC problem in Section 2. Section 3 presents the main result of this paper: two efficient algorithms to determine the optimal solution. In Section 4, we implement the proposed method and illustrate the results by simulations. Finally, we conclude the paper.

2. BACKGROUND

2.1 System Model

The configuration of a voltage source converter interconnected to the load via an inductive-capacitive (LC) filter is presented in Fig. 1. The system consists of the LC filter, the load (modeled as an independent current source), and the switching stage.

The state of the LC filter is described in stationary *abc* frame with state vector and dynamics

$$\begin{aligned} x &:= [\sqrt{L}I_{\mathrm{a}}\ \sqrt{L}I_{\mathrm{b}}\ \sqrt{L}I_{\mathrm{c}}\ \sqrt{C}V_{\mathrm{a}}\ \sqrt{C}V_{\mathrm{b}}\ \sqrt{C}V_{\mathrm{c}}]^T \\ \dot{x}(t) &= A_{\mathrm{c}}x(t) + B_{\mathrm{c}}s(t)V_{\mathrm{dc}} + F_{\mathrm{c}}I_{\mathrm{o}}(t) \end{aligned} \tag{1}$$

where I_p are the inductor currents, V_p are the capacitor voltages, $p \in \{\mathrm{a,b,c}\}$. L, C and V_{dc} are the filter inductance, capacitance and (constant) DC link voltage respectively. $I_{\mathrm{o}} = [I_{\mathrm{oa}}, I_{\mathrm{ob}}, I_{\mathrm{oc}}]^T \in \mathbb{R}^3$ are three-phase load currents, and $s = [s_{\mathrm{a}}, s_{\mathrm{b}}, s_{\mathrm{c}}]^T \in \{-1, 1\}^3$ represents the state of the converter switches. Expressions for the system matrices A_{c}, B_{c}, F_{c} can be found in (Almér et al., 2020).

2.2 MPC Formulation

The MPC problem of controlling (1) is nonlinear and non-convex, since the control input is confined to a discrete set. However, it was shown in (Almér et al., 2020), that under the assumption that the LC filter resonance frequency $c = 1/\sqrt{LC}$ satisfies $cT_{\mathrm{s}} \leq \pi$, where T_{s} is the sampling time, the nonlinear MPC problem can be equivalently formulated as a QCQP. The switches s_k are firstly expressed in terms of duty cycle and phase shift, then they are transformed into control input $v_{p,k}$ in another convex set via a bijective mapping. Denote the discretized state and load current $x_k = x(kT_{\mathrm{s}})$ and $I_{\mathrm{o},k} = I_{\mathrm{o}}(kT_{\mathrm{s}})$ respectively.

The QCQP takes the following form

$$\begin{array}{ll} \min\limits_{x_k, v_k} & \sum_{k=1}^{N_{\mathrm{p}}} (x_k - r_{\mathrm{ref},k})^T Q_{\mathrm{c}} (x_k - r_{\mathrm{ref},k}) \\ \text{s.t.} & x_{k+1} = Ax_k + FI_{\mathrm{o},k} + Mv_k, \quad k \in 0, \ldots, N_{\mathrm{p}} - 1 \\ & x_0 = x_{\mathrm{init}} \\ & \|v_{\mathrm{p},k} - r_1\|^2 \leq R^2 \\ & \|v_{\mathrm{p},k} - r_2\|^2 \leq R^2 \\ & k \in 0, \ldots, N_{\mathrm{p}} - 1, \quad p \in \mathrm{a,b,c} \end{array} \tag{2}$$

where Q_{c} is a positive definite matrix, N_{p} is the prediction horizon, $r_{\mathrm{ref,k}} \in \mathbb{R}^6$ is the reference signal, $v_k = [v_{\mathrm{a},k}, v_{\mathrm{b},k}, v_{\mathrm{c},k}]^T \in \mathbb{R}^6$, $r_1 = [0, 0.5]^T \in \mathbb{R}^2$, $r_2 = 0.5[\sin(cT_{\mathrm{s}}), -\cos(cT_{\mathrm{s}})]^T \in \mathbb{R}^2$ and $R = 0.5$. Expressions for the system matrices A, F, M can be found in (Almér et al., 2020).

3. PROPOSED ALGORITHMS

In this section, we introduce two algorithms based on the solvers OSQP and HPIPM for solving MPC problem in (2) efficiently.

3.1 Operator Splitting Method for QCQP

Recent research based on a particular version of ADMM, proposed in (Stellato et al., 2020; Banjac et al., 2017), shows that ADMM is effective for solving quadratic programs. Defining the variables of problem (2) as

$$x = [x_1, \ldots, x_{N_{\mathrm{p}}}, v_0, \ldots, v_{N_{\mathrm{p}}-1}]^T \in \mathbb{R}^{12N_{\mathrm{p}}},$$

the MPC problem (2) can be written into the following form:

$$\begin{array}{ll} \min\limits_{x} & \frac{1}{2}x^T Px + q^T x \\ \text{s.t.} & \bar{A}_1 x = b \\ & \bar{A}_2 x \in \boldsymbol{B} \end{array}$$

where

$$P = 2\begin{bmatrix} \boldsymbol{I}_{N_{\mathrm{p}}} \otimes Q_{\mathrm{c}} & \\ & \boldsymbol{I}_{N_{\mathrm{p}}} \otimes \boldsymbol{0}_{6\times 6} \end{bmatrix}$$

$$q = -2\begin{bmatrix} Q_{\mathrm{c}} r_{\mathrm{ref},1} \\ \vdots \\ Q_{\mathrm{c}} r_{\mathrm{ref,N_p}} \\ \boldsymbol{0}_{6N_{\mathrm{p}}\times 1} \end{bmatrix}, \quad b = \begin{bmatrix} Ax_0 + FI_{\mathrm{o},0} \\ FI_{\mathrm{o},1} \\ \vdots \\ FI_{\mathrm{o},N_{\mathrm{p}}-1} \end{bmatrix}$$

Algorithm 1 Operator splitting method for QCQP.

Require: Initial points x_0, z_0, y_0 and parameters $\rho > 0$, $\sigma > 0$, $\alpha \in (0, 2)$

repeat

$$(\tilde{x}_{k+1}, \tilde{z}_{k+1}) \leftarrow \underset{\bar{A}\tilde{x}=\tilde{z}}{\operatorname{argmin}} \Big\{ \tfrac{1}{2}\tilde{x}^T P \tilde{x} + q^T \tilde{x} + \tfrac{\sigma}{2}\|\tilde{x} - x_k\|_2^2 + \tfrac{\rho}{2}\|\tilde{z} - z_k + \tfrac{1}{\rho} y_k\|_2^2 \Big\}$$

$$x_{k+1} \leftarrow \alpha \tilde{x}_{k+1} + (1-\alpha) x_k$$

$$z_{k+1} \leftarrow \Pi_{\mathcal{C}}(\alpha \tilde{z}_{k+1} + (1-\alpha) z_k + \tfrac{1}{\rho} y_k)$$

$$y_{k+1} \leftarrow y_k + \rho(\alpha \tilde{z}_{k+1} + (1-\alpha) z_k - z_{k+1})$$

$$k \leftarrow k+1$$

until termination condition is satisfied

$$\bar{A}_1 = \left[\begin{array}{cccc:cccc} \boldsymbol{I}_6 & & & & -M & & & \\ -A & \boldsymbol{I}_6 & & & & -M & & \\ & \ddots & \ddots & & & & \ddots & \\ & & -A & \boldsymbol{I}_6 & & & & -M \end{array}\right]_{6N_\mathrm{p} \times 12N_\mathrm{p}}$$

$$\bar{A}_2 = \left[\begin{array}{c:c} \mathbf{0}_{6N_\mathrm{p} \times 6N_\mathrm{p}} & \boldsymbol{I}_{6N_\mathrm{p}} \\ \hdashline \mathbf{0}_{6N_\mathrm{p} \times 6N_\mathrm{p}} & \boldsymbol{I}_{6N_\mathrm{p}} \end{array}\right]$$

$$\boldsymbol{B} \coloneqq B_1 \times \ldots \times B_1 \times B_2 \times \ldots \times B_2 \subseteq \mathbb{R}^{6N_\mathrm{p}+6N_\mathrm{p}}$$
$$B_1 \coloneqq \{v \in \mathbb{R}^2 \mid \|v - r_1\|^2 \leq R^2\}$$
$$B_2 \coloneqq \{v \in \mathbb{R}^2 \mid \|v - r_2\|^2 \leq R^2\}.$$

and where $\otimes$ and $\times$ denote the Kronecker and Cartesian products, respectively. $\boldsymbol{I}_\mathrm{m}$ is identity matrix and $\mathbf{0}_{\mathrm{m}\times\mathrm{n}}$ is zero matrix.

Note that the problem above can be written in the following form:

$$\begin{aligned} \min_x \quad & \tfrac{1}{2}x^T P x + q^T x \\ \text{s.t.} \quad & \bar{A}x \in \mathcal{C} \end{aligned}$$

where

$$\bar{A} = \begin{bmatrix} \bar{A}_1 \\ \bar{A}_2 \end{bmatrix} \quad \text{and} \quad \mathcal{C} \coloneqq \{b\} \times \boldsymbol{B}.$$

The formulation above matches the one in (Stellato et al., 2020, §1.1), and thus we can employ the same splitting method, which is summarized in Algorithm 1. In Algorithm 1, the operator $\Pi_{\mathcal{C}}$ denotes the Euclidean projection onto the set $\mathcal{C}$. Since $\mathcal{C}$ is given as a Cartesian product of multiple sets, we can evaluate $\Pi_{\mathcal{C}}(z)$ by computing projections onto the singleton $\{b\}$ and the balls B_1 and B_2. The projection onto the ball B_i has the following closed-form solution:

$$\Pi_{B_i}(v) = \begin{cases} v & \|v - r_i\|_2 \leq R \\ \frac{v - r_i}{\|v - r_i\|_2} R + r_i & \text{otherwise} \end{cases},$$

which is illustrated in Fig. 2. The termination conditions for Algorithm 1 can be found in (Stellato et al., 2020, §3.4).

3.2 Riccati-Based Interior-Point Method for QCQP

An alternative approach to solve the quadratically constrained MPC problem in (2) is to extend the Riccati-based interior-point method proposed in (Frison and Jørgensen, 2013; Frison et al., 2014). Consider the MPC problem in (2), we define the decision variables $w = [u_0, x_1, u_1, ..., , u_{N_\mathrm{p}-1}, x_{N_\mathrm{p}}]^T \in \mathbb{R}^{12N_\mathrm{p}}$, dual variable $\pi = [\pi_1, \pi_2, ..., \pi_{N_\mathrm{p}}]^T \in \mathbb{R}^{6N_\mathrm{p}}$ associated with equality constraints and $\lambda = [\lambda_1, \lambda_2, ..., \lambda_{6N_\mathrm{p}}]^T \in \mathbb{R}^{6N_\mathrm{p}}$ associated with

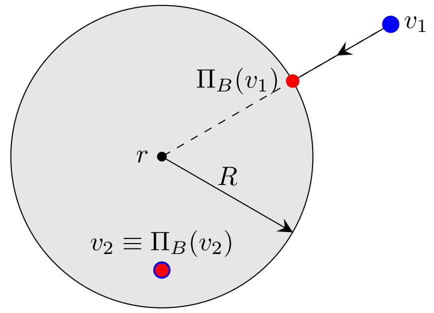

Fig. 2. The Euclidean projection onto the ball B centered at r and with radius R.

quadratic constraints. Furthermore, $t = [t_1, t_2, ..., t_{6N_\mathrm{p}}]^T \in \mathbb{R}^{6N_\mathrm{p}}$ are introduced as slack variables. The relaxed KKT conditions read as

$$\mathbb{F}(w, \pi, \lambda, t) = \begin{bmatrix} (\tilde{H} + C_\lambda)w - \check{A}^T \pi + g \\ -\check{A}w + b \\ \|v_{a,0} - r_1\|^2 - R^2 + t_1 \\ \|v_{a,0} - r_2\|^2 - R^2 + t_2 \\ \|v_{b,0} - r_1\|^2 - R^2 + t_3 \\ \|v_{b,0} - r_2\|^2 - R^2 + t_4 \\ \vdots \\ \|v_{c,N_\mathrm{p}-1} - r_1\|^2 - R^2 + t_{6N_\mathrm{p}-1} \\ \|v_{c,N_\mathrm{p}-1} - r_2\|^2 - R^2 + t_{6N_\mathrm{p}} \\ T\Lambda e \end{bmatrix} = 0 \quad (3)$$

where we define the following quantities:

$$\tilde{H} + C_\lambda = 2 \begin{bmatrix} \mathcal{K}_1 & & & & \\ & Q_\mathrm{c} & & & \\ & & \ddots & & \\ & & & \mathcal{K}_{N_\mathrm{p}} & \\ & & & & Q_\mathrm{c} \end{bmatrix}_{12N_\mathrm{p} \times 12N_\mathrm{p}}$$

$$\mathcal{K}_i = \begin{bmatrix} \sum_{j=1}^{2} \lambda_{6(i-1)+j} \boldsymbol{I}_2 & & \\ & \sum_{j=3}^{4} \lambda_{6(i-1)+j} \boldsymbol{I}_2 & \\ & & \sum_{j=5}^{6} \lambda_{6(i-1)+j} \boldsymbol{I}_2 \end{bmatrix}$$

$$i = 1, 2, .., N_\mathrm{p}$$

$$g = -2 \begin{bmatrix} \mathcal{L}_1 \\ Q_\mathrm{c} r_{\mathrm{ref},1} \\ \vdots \\ \mathcal{L}_{N_\mathrm{p}} \\ Q_\mathrm{c} r_{\mathrm{ref},\mathrm{N_p}} \end{bmatrix}, b = \begin{bmatrix} Ax_0 + FI_{o,0} \\ FI_{o,1} \\ \vdots \\ FI_{o,N_\mathrm{p}-1} \end{bmatrix}$$

$$\mathcal{L}_i = \begin{bmatrix} \lambda_{6(i-1)+1} r_1 + \lambda_{6(i-1)+2} r_2 \\ \lambda_{6(i-1)+3} r_1 + \lambda_{6(i-1)+4} r_2 \\ \lambda_{6(i-1)+5} r_1 + \lambda_{6(i-1)+6} r_2 \end{bmatrix}, i = 1, 2, .., N_\mathrm{p}$$

$$\check{A} = \begin{bmatrix} -M & \boldsymbol{I}_6 & & & & \\ & -A & -M & \boldsymbol{I}_6 & & \\ & & & \ddots & \ddots & \\ & & & -A & -M & \boldsymbol{I}_6 \end{bmatrix}_{6N_\mathrm{p} \times 12N_\mathrm{p}}$$

$$T = \begin{bmatrix} t_1 & & \\ & \ddots & \\ & & t_{6N_\mathrm{p}} \end{bmatrix},\ \Lambda = \begin{bmatrix} \lambda_1 & & \\ & \ddots & \\ & & \lambda_{6N_\mathrm{p}} \end{bmatrix},\ e = \begin{bmatrix} 1 \\ \vdots \\ 1 \end{bmatrix}_{6N_\mathrm{p}}$$

Furthermore, we define the barrier parameter $\mu \geq 0$ and centering parameter $\sigma \in [0,1]$. The values of μ and σ define the central path, which is a trajectory towards the solution of the problem as $\mu\sigma$ tends to zero. Applying Newton's method to (3), at each iteration k, we have that

$$\left[\begin{array}{c|c|c|c} \tilde{H} + C_{\lambda_k} & -\check{A}^T & C_{u_k}^T & \\ \hline -\check{A} & & & \\ \hline C_{u_k} & & & \boldsymbol{I}_{6N_\mathrm{p}} \\ \hline & & T_k & \Lambda_k \end{array}\right] \begin{bmatrix} \Delta w_k \\ \Delta \pi_k \\ \Delta \lambda_k \\ \Delta t_k \end{bmatrix} = \begin{bmatrix} -r_{\tilde{H}_k} \\ -r_{\pi_k} \\ -r_{\lambda_k} \\ -r_{t_k} \end{bmatrix} \tag{4}$$

where

$$C_u = 2 \begin{bmatrix} \mathcal{U}_1 & \mathbf{0}_{6\times 6} & & \\ & & \ddots & \\ & & & \mathcal{U}_{N_\mathrm{p}} & \mathbf{0}_{6\times 6} \end{bmatrix}_{6N_\mathrm{p}\times 12 N_\mathrm{p}}$$

$$\mathcal{U}_i = \begin{bmatrix} (v_{a,i-1} - r_1)^T & & \\ (v_{a,i-1} - r_2)^T & & \\ & (v_{b,i-1} - r_1)^T & \\ & (v_{b,i-1} - r_2)^T & \\ & & (v_{c,i-1} - r_1)^T \\ & & (v_{c,i-1} - r_2)^T \end{bmatrix}_{6\times 6}$$

$$i = 1, 2, .., N_\mathrm{p}$$

$$r_{\tilde{H}} = (\tilde{H} + C_\lambda) w - \check{A}^T \pi + g$$

$$r_\pi = -\check{A} w + b$$

$$r_\lambda = \begin{bmatrix} \|v_{a,0} - r_1\|^2 - R^2 + t_1 \\ \|v_{a,0} - r_2\|^2 - R^2 + t_2 \\ \|v_{b,0} - r_1\|^2 - R^2 + t_3 \\ \|v_{b,0} - r_2\|^2 - R^2 + t_4 \\ \vdots \\ \|v_{c,N_\mathrm{p}-1} - r_1\|^2 - R^2 + t_{6N_\mathrm{p}-1} \\ \|v_{c,N_\mathrm{p}-1} - r_2\|^2 - R^2 + t_{6N_\mathrm{p}} \end{bmatrix}$$

$$r_t = T\Lambda e - \mu\sigma e.$$

Finally, we can define the primal residuals ϵ^{prim} and dual residual ϵ^{dual} as,

$$\epsilon^{\mathrm{prim}} = \|[r_\pi, r_\lambda]^T\|_\infty \tag{5}$$

$$\epsilon^{\mathrm{dual}} = \|r_{\tilde{H}}\|_\infty. \tag{6}$$

Now we can rewrite (4) into symmetric KKT system by Schur complement, *i.e.*,

$$\left[\begin{array}{c|c} H + C_{\lambda_k} + C_{u_k}^T (T_k)^{-1} \Lambda_k C_{u_k} & -\check{A}^T \\ \hline -\check{A} & \end{array}\right] \begin{bmatrix} \Delta w_k \\ \Delta \pi_k \end{bmatrix} = -\begin{bmatrix} r_{\hat{H}_k} \\ r_{\pi_k} \end{bmatrix}, \tag{7}$$

where

$$r_{\hat{H}_k} = r_{H_k} - C_{u_k}^T (T_k)^{-1} r_{t_k} + C_{u_k}^T (T_k)^{-1} \Lambda_k r_{\lambda_k}$$

$$\Delta t_k = -r_{\lambda_k} - C_{u_k} \Delta w_k$$

$$\Delta \lambda_k = -T_k^{-1} (r_{t_k} + \Lambda_k \Delta t_k).$$

Next, the decision variables are rewritten in

$$\Delta = [\Delta u_0, \Delta\pi_1, \Delta x_1, \ldots, \Delta u_{N_\mathrm{p}-1}, \Delta \pi_{N_\mathrm{p}}, \Delta x_{N_\mathrm{p}}]^T,$$

the corresponding perturbed KKT system (7) consist of the band-diagonal matrix K_{band} and right-hand side

Algorithm 2 Riccati-based interior-point method for QCQP.

Require: $(w_0, \pi_0, \lambda_0, t_0)$ with $(\lambda_0, t_0) \geq 0$;
for $k = 1, 2, \ldots$ **do**
  $(w, \pi, \lambda, t) \leftarrow (w_k, \pi_k, \lambda_k, t_k)$
  $(\Delta w^{\mathrm{aff}}, \Delta \pi^{\mathrm{aff}}, \Delta \lambda^{\mathrm{aff}}, \Delta t^{\mathrm{aff}}) \leftarrow$ solve (8) with $\sigma = 0$ in Alg.3
  $\mu \leftarrow \lambda_k^T t_k / (6N_\mathrm{p})$
  $\tilde{\alpha}_{\mathrm{aff}} \leftarrow \max\{\alpha \in [0,1] \mid (\lambda_k, t_k) + \alpha(\Delta\lambda^{\mathrm{aff}}, \Delta t^{\mathrm{aff}}) \geq 0\}$
  $\mu_{\mathrm{aff}} \leftarrow (\lambda_k + \tilde{\alpha}_{\mathrm{aff}} \Delta \lambda^{\mathrm{aff}})^T (t_k + \tilde{\alpha}_{\mathrm{aff}} \Delta t^{\mathrm{aff}}) / (6N_\mathrm{p})$
  $\sigma \leftarrow (\mu_{\mathrm{aff}} / \mu)^3$
  $(\Delta w, \Delta \pi, \Delta \lambda, \Delta t) \leftarrow$ solve (8) in Alg.3
  Choose $\tau_k \in (0,1)$
  $\alpha_{\tau_k}^{\mathrm{prim}} \leftarrow \max\{\alpha \in [0,1] \mid t_k + \alpha \Delta t \geq (1 - \tau_k) t_k\}$
  $\alpha_{\tau_k}^{\mathrm{dual}} \leftarrow \max\{\alpha \in [0,1] \mid \lambda_k + \alpha \Delta\lambda \geq (1 - \tau_k)\lambda_k\}$
  $\tilde{\alpha} \leftarrow \min(\alpha_{\tau_k}^{\mathrm{prim}}, \alpha_{\tau_k}^{\mathrm{dual}})$
  $(w_{k+1}, \pi_{k+1}, \lambda_{k+1}, t_{k+1}) \leftarrow (w_k, \pi_k, \lambda_k, t_k) + \tilde{\alpha}(\Delta w_k, \Delta \pi_k, \Delta \lambda_k, \Delta t_k)$
  Update $\epsilon_k^{\mathrm{prim}}$ and $\epsilon_k^{\mathrm{dual}}$, check termination conditions.
end for

vector r_{band}, whose structure coincides with the unconstrained one in (Frison and Jørgensen, 2013),

$$K_{\mathrm{band}} \Delta = r_{\mathrm{band}} \tag{8}$$

where

$$K_{\mathrm{band}} = \begin{bmatrix} \boldsymbol{R}_0 & M^T & & & & & & \\ M & & -\boldsymbol{I}_6 & & & & & \\ & -\boldsymbol{I}_6 & \boldsymbol{Q}_1 & \boldsymbol{S}_1^T & A^T & & & \\ & & \boldsymbol{S}_1 & \boldsymbol{R}_1 & M^T & & & \\ & & A & M & & -\boldsymbol{I}_6 & & \\ & & & & -\boldsymbol{I}_6 & \boldsymbol{Q}_2 & \ddots & \\ & & & & & \ddots & \ddots & -\boldsymbol{I}_6 \\ & & & & & & -\boldsymbol{I}_6 & \boldsymbol{P} \end{bmatrix}$$

$$r_{\mathrm{band}} = -[\tilde{s}_0, \tilde{b}_0, \tilde{q}_1, \ldots, \tilde{s}_{N_\mathrm{p}-1}, \tilde{b}_{N_\mathrm{p}-1}, \tilde{q}_{N_\mathrm{p}}]^T.$$

We describe the full predictor-corrector algorithm in Algorithm 2. The linear system solution by backward Riccati factorization is listed in Algorithm 3. Note that 'Chol' denotes Cholesky factorization and β and Θ are lower triangular matrices. Notice that, at submission time, the support for QCQPs has been added to HPIPM independently of our work.

4. IMPLEMENTATION

We now discuss numerical results and compare the performance of different algorithms, including some commercial solvers. The implementation focuses on small to medium size problems. All the demos are tested on an Intel Core i7 6700HQ @2.6GHz processor, the compiler is Visual Studio C++ on Linux 64 bit. The system parameters are summarized in Tab. 1.

As it can be seen in Algorithm 1, we need to choose parameters ρ, σ, α for the splitting method. As suggested in (Stellato et al., 2020), we set $\sigma = 10^{-6}$ and $\alpha = 1.6$. In addition, we obtain good numerical performance for $\rho = 5$.

In the primal-dual interior point method, the only parameter we need to determine is τ. We could choose an adaptive τ_k that approaches 1 as the iterates approach the solution

Algorithm 3 Backward Riccati for solving KKT system.

Require: KKT system and N_{p};
  Set $\beta_{N_{\mathrm{p}}} \leftarrow \mathrm{Chol}(\boldsymbol{P})$
  for $n = N_{\mathrm{p}} - 1 \rightarrow 1$ **do**
    $\Sigma \leftarrow \beta_{n+1}^T [M \;\; A]$
    if $n = 0$ **then**
      $\boldsymbol{S}_0 = \boldsymbol{0}_{6\times 6}, \boldsymbol{Q}_0 = 2Q_{\mathrm{c}}$
    end if
    $\mathcal{M} \leftarrow \Sigma^T\Sigma + \begin{bmatrix} \boldsymbol{R}_n & \boldsymbol{S}_n \\ \boldsymbol{S}_n^T & \boldsymbol{Q}_n \end{bmatrix}$
    $\begin{bmatrix} \Theta_n & \\ L_n^T & \beta_n \end{bmatrix} \leftarrow \mathrm{Chol}(\mathcal{M})$
  end for
  Set $p_{N_{\mathrm{p}}} \leftarrow \tilde{q}_{N_{\mathrm{p}}}$
  for $n = N_{\mathrm{p}} - 1 \rightarrow 0$ **do**
    $l_n \leftarrow (\Theta_n^T)^{-1}(\tilde{s}_n + M^T(\beta_{n+1}^T\beta_{n+1}\tilde{b}_n + p_{n+1}))$
    $p_n \leftarrow \tilde{q}_n + A^T(\beta_{n+1}^T\beta_{n+1}\tilde{b}_n + p_{n+1}) - L_n^T l_n$
  end for
  for $n = 0 \rightarrow N_{\mathrm{p}} - 1$ **do**
    $\Delta u_n \leftarrow -(\Theta_n^T)^{-1}(L_n\Delta x_n + l_n)$
    $\Delta x_{n+1} \leftarrow A\Delta x_n + M\Delta u_n + \tilde{b}_n$
    $\Delta\pi_{n+1} \leftarrow L_{n+1}^T L_{n+1}\Delta x_{n+1} + p_{n+1}$
  end for

Table 1. Simulation settings.

System parameters	Values
Inductance of coil L	0.736 p.u.
Capacitance C	3.336 p.u.
Nominal DC voltage V_{dc}	0.727 p.u.
Nominal load current amplitude I_o	0.591 p.u.
Sampling (and Control) period T_s	310 μs
Prediction horizon N_{p}	2
Penalties in Q_{c} for inverter current error	1/30
Penalties in Q_{c} for capacitor voltage error	10/30

or directly set it to a constant value $\tau_k \in [0.9, 1]$. We record the averaged number of iterations for high accuracy solution over 100 random initial points. The results are shown in Fig. 3, the choice of adaptive τ_k, *i.e.*,

$$\tau_k = 1 - 0.01e^{-(k-1)}, \quad k = 1, 2 \ldots \tag{9}$$

speeds up convergence.

Next, we perform the comparison with other commercial interior point solvers GUROBI 7.5.1, MOSEK 8.0 and open-source solvers SDPT3 4.0 and ECOS. We execute all the methods with default settings. The fast gradient method for real-time MPC (Richter et al. (2012)) is not considered here since it requires approximation of the ellipsoidal constraints by boxes and cannot obtain exact solution.

For each solver, the averaged computation time is computed for 1000 random initial points under different accuracies. As shown in Fig. 4, the proposed operator splitting method and Riccati method are suitable for the case of low-accuracy applications like embedded control (*e.g.* tolerances of 10^{-3} to 10^{-4} in Fig. 4) and outperform the competing solvers, while Riccati method performs better than all others when a high accuracy is required.

Finally, warm-starting can significantly improve computation times in MPC. In particular, we initialize the iterates

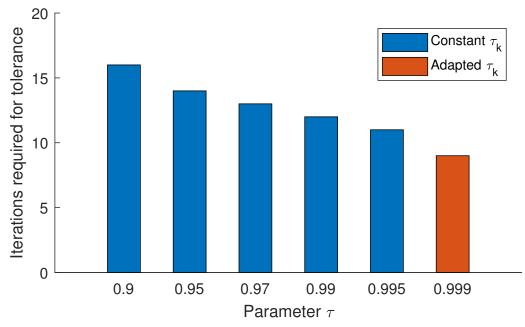

Fig. 3. The number of iterations reaches tolerance with different values of τ.

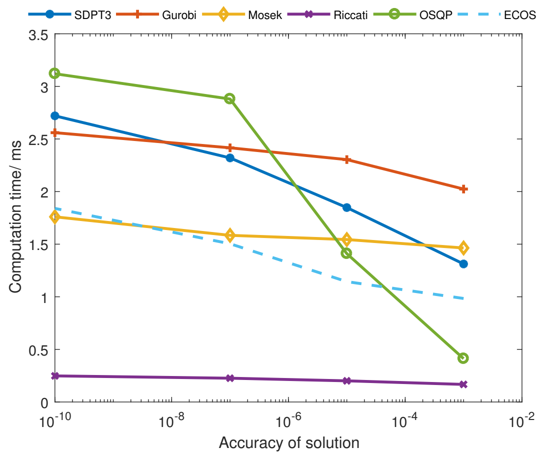

Fig. 4. Computation time vs solution accuracy for proposed methods and solvers.

of our methods to the solution of the previous problem and compute the averaged computation time. The obtained speedup is shown in Fig. 5.

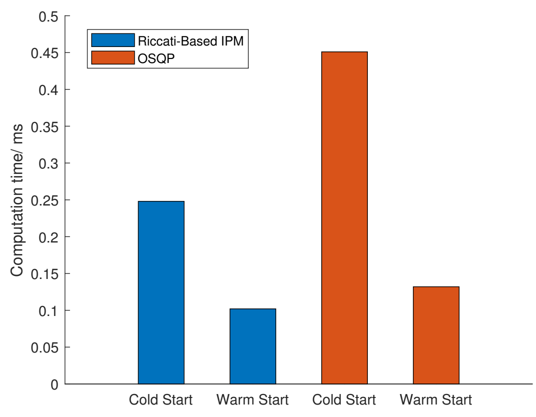

Fig. 5. Comparison of warm-start performance given low accuracy.

5. CONCLUSION

Motivated by a new formulation of a power electronics MPC problem, we presented two tailored optimization algorithms for real-time control using QCQP. In the ADMM framework, inspired by a novel operator splitting method, the quadratic constraints and the linear dynamics are reformulated into an easy-to-project set. The other formulation based on the primal-dual interior-point method uses a Riccati-type factorization to solve the KKT system efficiently. We present several simulation results of an MPC tracking problem and show that our tailored QCQP algorithms outperform off-the-shelf solvers. In a future study, techniques like preconditioning and heuristic methods could be integrated into OSQP to further reduce the number of iterations. Furthermore, a real-world embedded control setup is envisaged.

REFERENCES

Almér, S., Frick, D., Torrisi, G., and Mariéthoz, S. (2020). Predictive converter control: Hidden convexity and real-time quadratically constrained optimization. *IEEE Transactions on Control Systems Technology*, 1–8. doi: 10.1109/TCST.2019.2963253.

Almér, S., Mariéthoz, S., and Morari, M. (2013). Sampled Data Model Predictive Control of a Voltage Source Inverter for Reduced Harmonic Distortion. *IEEE Transactions on Control Systems Technology*, 21(5), 1907–1915.

Almér, S., Mariéthoz, S., and Morari, M. (2015). Dynamic Phasor Model Predictive Control of Switched Mode Power Converters. *IEEE Transactions on Control Systems Technology*, 23(1), 349–356.

Banjac, G., Goulart, P., Stellato, B., and Boyd, S. (2019). Infeasibility Detection in the Alternating Direction Method of Multipliers for Convex Optimization. *Journal of Optimization Theory and Applications*, 183(2), 490–519.

Banjac, G., Stellato, B., Moehle, N., Goulart, P., Bemporad, A., and Boyd, S. (2017). Embedded Code Generation Using the OSQP Solver. In *IEEE Conference on Decision and Control (CDC)*, 1906–1911.

Boyd, S., Parikh, N., Chu, E., Peleato, B., and Eckstein, J. (2011). Distributed optimization and statistical learning via the alternating direction method of multipliers. *Foundations and Trends in Machine Learning*, 3(1), 1–122. doi:10.1561/2200000016.

C.V.Rao, S.J.Wright, and J.B.Rawlings (1998). Application of interior point methods to model predictive control. *JOURNAL OF OPTIMIZATION THEORY AND APPLICATIONS*, 99(3), 723–757.

Domahidi, A., Chu, E., and Boyd, S. (2013). ECOS: An SOCP solver for embedded systems. In *IEEE European Control Conference (ECC)*, 3071–3076.

Domahidi, A., Zgraggen, A.U., Zeilinger, M.N., Morari, M., and Jones, C.N. (2012). Efficient interior point methods for multistage problems arising in receding horizon control. In *IEEE Conference on Decision and Control*, 668–674.

Douglas, J. and Rachford, H.H. (1956). On the Numerical Solution of Heat Conduction Problems in Two and Three Space Variables. *Transactions of the American mathematical Society*, 82(2), 421–439.

Eckstein, J. and Bertsekas, D.P. (1992). On the Douglas-Rachford Splitting Method and the Proximal Point Algorithm for Maximal Monotone Operators. *Mathematical Programming*, 55(1-3), 293–318.

Ferreau, H.J., Almér, S., Verschueren, R., Diehl, M., Frick, D., Domahidi, A., Jerez, J.L., Stathopoulos, G., and Jones, C. (2017). Embedded Optimization Methods for Industrial Automatic Control. *IFAC-PapersOnLine*, 50(1), 13194–13209.

Frison, G. and Jørgensen, J.B. (2013). Efficient Implementation of the Riccati Recursion for Solving Linear-Quadratic Control Problems. In *IEEE International Conference on Control Applications (CCA)*, 1117–1122.

Frison, G., Kouzoupis, D., Sartor, T., Zanelli, A., and Diehl, M. (2018). BLASFEO: Basic Linear Algebra Subroutines for Embedded Optimization. *ACM Transactions on Mathematical Software (TOMS)*, 44(4), 42.

Frison, G., Sørensen, H.H.B., Dammann, B., and Jørgensen, J.B. (2014). High-Performance Small-Scale Solvers for Linear Model Predictive Control. In *IEEE European Control Conference (ECC)*, 128–133.

Gabay, D. and Mercier, B. (1976). A Dual Algorithm for the Solution of Nonlinear Variational Problems via Finite Element Approximation. *Computers & mathematics with applications*, 2(1), 17–40.

Glowinski, R. (1984). *Numerical Methods for Nonlinear Variational Problems*. Springer-Verlag, New York.

Hokayem, P., Geyer, T., and Oikonomou, N. (2014). Active Damping for Model Predictive Pulse Pattern Control. In *IEEE Energy Conversion Congress and Exposition (ECCE)*, 1220–1227.

Lions, P.L. and Mercier, B. (1979). Splitting Algorithms for the Sum of Two Nonlinear Operators. *SIAM Journal on Numerical Analysis*, 16(6), 964–979.

Mehrotra, S. (1992). On the Implementation of a Primal-Dual Interior Point Method. *SIAM Journal on optimization*, 2(4), 575–601.

Parvez, I., Abdul, F., and Sarwat, A.I. (2016). A Location based Key Management System for Advanced Metering Infrastructure of Smart Grid. In *IEEE Green Technologies Conference (GreenTech)*, 62–67.

Richter, S., Colin, J., and Morari, M. (2012). Computational Complexity Certification for Real-Time MPC With Input Constraints Based on the Fast Gradient Method. *IEEE Transactions on Automatic Control*, 57(6), 1391–1403.

Richter, S., Geyer, T., and Morari, M. (2016). Resource-Efficient Gradient Methods for Model Predictive Pulse Pattern Control on an FPGA. *IEEE Transactions on control systems technology*, 25(3), 828–841.

Spudić, V. and Geyer, T. (2017). Fast Control of a Modular Multilevel Converter STATCOM Using Optimized Pulse Patterns. In *IEEE Energy Conversion Congress and Exposition (ECCE)*, 2707–2714.

Stellato, B., Banjac, G., Goulart, P., Bemporad, A., and Boyd, S. (2020). OSQP: An Operator Splitting Solver for Quadratic Programs. *Mathematical Programming Computation*.

Vazquez, S., Rodriguez, J., Rivera, M., Franquelo, L.G., and Norambuena, M. (2016). Model Predictive Control for Power Converters and Drives: Advances and Trends. *IEEE Transactions on Industrial Electronics*, 64(2), 935–947.

Wright, S.J. (1997). *Primal-Dual Interior-Point Methods*, volume 54. Siam.